Excitation of $n=2$ States in Helium by Electron Bombardment*

HELEN K. HOLT† AND R. KROTKOV
Gibbs Laboratory, Yale University, New Haven, Connecticut
(Received 8 November 1965)

We have measured the total cross section for excitation of the 2^1S state in helium by electron bombardment, together with the sum of the 2^3S and 2^3P cross sections. Singlet metastable atoms were distinguished from triplet ones by quenching the singlets in an electric field. An estimate of the 2^3P cross section is made. All measurements were relative to the peak of the 2^3S cross section, and covered the energy range 19.8 to 23.2 eV. Assuming a value of $(3.0\pm0.7)\times10^{-18}$ cm^2 for this peak, the 2^1S cross section was found to rise from threshold to a plateau at $(1.0\pm0.3)\times10^{-18}$ cm^2. The 2^3P cross section rises steadily from threshold to $(3.0\pm1.0)\times10^{-18}$ cm^2 at 23.2 eV. Measurements were also made of the relative populations of the magnetic substates of the 2^3S state. These are related to the polarization of the collision light emitted in the $2^3P\rightarrow2^3S$ decay and were motivated by the well-known polarization anomaly. For about 2 V above the 2^3P threshold the measured tensor polarization has the constant value -0.06 ± 0.06, which may be compared with a predicted threshold value of -0.55. This result is interpreted in terms of resonance structure.

I. INTRODUCTION

MANY studies have been made of what happens when electrons bombard helium. The subject is interesting because there is some hope of interpreting the results theoretically. In addition, cross sections are often required for other reasons, for example, in the study of lasers, in astrophysics, or for practical engineering purposes. At the present time, there is much interest in the resonance structure which has been discovered.

Our work concerns electronic excitation from the ground state to the levels with principal quantum number $n=2$. These are shown in Fig. 1. As is well known, the 2^3S and 2^1S states are metastable, having lifetimes greater than about 0.14 sec for the 2^1S, and 10^5 sec for the 2^3S, state.[1] In our experiments the electron energy was kept below the threshold for production of $n=3$ states; i.e., the energy range covered was 19.8–22.7 eV. We have measured the total cross section for exciting the metastable 2^1S state, and the sum of the the total cross sections for exciting the 2^3S and 2^3P states. An estimate was obtained for the 2^3P cross section. In addition, by filtering the beam of excited atoms in an inhomogeneous magnetic field, total cross sections were obtained for producing 2^3S atoms in states with magnetic quantum numbers $M_s=+1$, 0, and -1 (relative to a quantization axis taken along the electron velocity). Such measurements can distinguish, at least partially, between resonances of different angular momenta and in this sense can give information similar to that obtainable from angular distributions.

Only relative cross sections were measured. Absolute values quoted were obtained by making measurements relative to the peak of the 2^3S cross section, which has been measured absolutely by a number of workers.[2,3] The energy resolution of our electron beam was about 0.5 eV.

As a check on agreement with the results of other experimenters, the sum of our two measured cross sections (2^1S together with 2^3S plus 2^3P) may be compared with measurements of the total metastable cross section made by other workers over our energy range. This is done in Sec. 3A. The agreement is satisfactory (see Fig. 7).

In Sec. 3B the measurement of the 2^1S total cross section will be compared with theoretical calculations of Marriott[4] and of Massey and Moiseiwitsch.[5] The agreement is fair (better than a factor 3). No other direct measurements of this cross section have been reported to our knowledge. In Sec. 3C our estimate of the 2^3P cross section will be compared with theoretical calculations of Massey and Moiseiwitsch.[6] The agreement is poor but the comparison is perhaps invalid since the calculation was really intended for higher energies. No direct measurements of either the 2^3S or 2^3P total cross sections or their sum have been reported over our energy range.

The measurements on magnetic quantum number dependence of the cross section for producing 2^3S atoms yield information equivalent to a measurement of the polarization of light emitted during the $2^3P\rightarrow2^3S$ transition, and were motivated by the well-known threshold "anomaly" in the polarization of collision light. Our results are also "anomalous" in the same sense as the polarization is; in view of the known resonance structure in the e^-+He scattering the "anomaly" is probably not surprising. This is discussed in Sec. 4.

It may be useful to compare our measurements with related ones in the literature. These may conveniently be grouped by the end products measured. In the first

* This research was supported in part by the National Aeronautics and Space Administration.

† This paper is based on a thesis submitted by Helen K. Holt to Yale University in partial fulfillment of the requirements for the Ph.D. degree.

[1] G. Breit and E. Teller, Astrophys. J. **91**, 215 (1940).

[2] G. J. Schulz and R. E. Fox, Phys. Rev. **106**, 1179 (1957).

[3] R. J. Fleming and G. S. Higginson, Proc. Phys. Soc. (London) **84**, 531 (1964).

[4] R. Marriott in *Atomic Collision Processes*, edited by M. R. C. McDowell (North-Holland Publishing Company, Amsterdam, 1964), p. 114.

[5] H. S. W. Massey and B. L. Moiseiwitsch, Proc. Roy. Soc. (London) **A227**, 38 (1954).

[6] H. S. W. Massey and B. L. Moiseiwitsch, Proc. Roy. Soc. (London) **A258**, 147 (1960).

place, there are observations of optical excitation functions.[7–9] At energies greater than about 3 eV above the 2^3S threshold, interpretation of the measurements is complicated by cascade effects, and analysis is required to obtain a cross-section curve for exciting a specific level of interest. However, in the energy range 2^3S threshold to threshold plus 2.90 eV the only triplet line is that at 10 830 Å ($2^3P \rightarrow 2^3S$), so a measurement of this excitation function in this energy range would yield the 2^3P excitation cross section. Similar comments apply to the $2^1P \rightarrow 2^1S$ transition at 20 581 Å. However, no such measurements have been reported.

Another group of measurements are concerned with production of the metastable states,[2,3,10–12] which are relatively easy to detect. Over the limited energy range 2^3S threshold to 2^1S threshold (19.82 to 20.61 V), these yield the total 2^3S cross section. However, at higher energies, the yield of metastable atoms also becomes complicated by cascade effects. Our measurements of the 2^1S and 2^3S+2^3P cross sections may be regarded as an extension of these, with the 2^1S metastable state being separated out from the 2^3S.

Cascade effects are eliminated in experiments in which the inelastically scattered electrons are energy-analyzed.[13,14] The 2^3S cross section has been measured this way with good energy resolution. The experiments reported so far give differential cross sections at two angles. Our measurements are of the total cross sections.

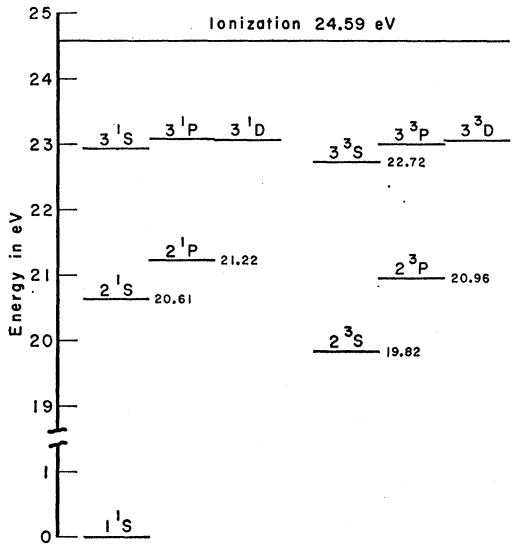

FIG. 1. Low-lying energy levels of He. The numbers beside a level give its energy in eV relative to the ground state.

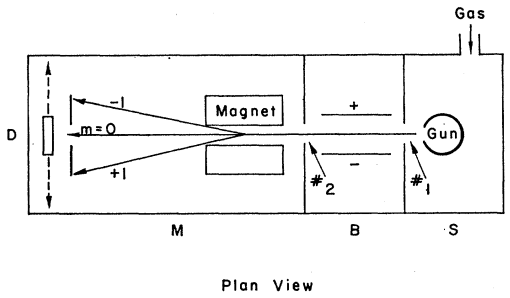

FIG. 2. Schematic diagram of the apparatus. Dimensions are given in Table I.

2. APPARATUS

A. General Description

A schematic diagram of the apparatus in plan view is shown in Fig. 2. The vacuum system shown in this figure consists of three parts: a source chamber (S), a buffer chamber (B), and a main chamber (M), each separately pumped.

The source chamber contained the electron gun and was filled with helium. At thermal velocities ($\sim 10^5$ cm/sec) an atom excited to an optically decaying state travelled a very short distance ($\sim 10^{-2}$ cm) before decaying with a typical lifetime ($\sim 10^{-7}$ sec). Hence the electron beam may be thought of as a source of ground state and metastable atoms. The angular distribution of these atoms was essentially isotropic with only small deviations from this condition because of momentum transfer effects.[15]

Those atoms going in the proper direction passed through two slits, 1 and 2, in the walls of the buffer chamber and eventually passed through a detector slit and impinged on the detector D. On the way they passed through an electric field region in the buffer chamber and through a magnetic field gradient in the main chamber. The purpose of the electric field was to quench the singlet metastables, while the purpose of the magnet was to separate spatially the triplet metastables into three beams corresponding to magnetic quantum numbers $M_s=\pm 1$ and 0.

The electron beam was directed downward while the electric field vector was horizontal, as was the direction of deflection in the magnet. The dimensions of the apparatus are listed in Table I. The time taken by the metastable atoms to traverse the distance from gun to

TABLE I. Distances from center of interaction volume.

Slit No. 1 (0.015×0.635 cm)	4.8 cm
Slit No. 2 (0.015×0.635 cm)	18.8 cm
Detector slit (0.025×1.59 cm)	91.1 cm

[7] A. H. Gabriel and D. W. O. Heddle, Proc. Roy. Soc. (London) A258, 123 (1960).
[8] D. T. Stewart and E. Gabathuler, Proc. Phys. Soc. (London) 74, 473 (1959).
[9] C. Smit, H. G. M. Heideman, and J. A. Smit, Physica 29, 245 (1963).
[10] R. Dorrestein, Physica 9, 447 (1942).
[11] R. H. McFarland, Phys. Rev. 136, A1240 (1964).
[12] H. Maier-Leibnitz, Z. Physik 95, 499 (1935).
[13] G. J. Schulz and J. W. Philbrick, Phys. Rev. Letters 13, 477 (1964).
[14] G. E. Chamberlain, Phys. Rev. Letters 14, 581 (1965); G. E. Chamberlain and H. G. M. Heideman, *ibid.* 15, 337 (1965).

detector was about 10^{-3} sec, which is much shorter than their lifetime ($\gtrsim$0.14 sec).

The source chamber pump was CVC-type PMC 1440, with a liquid-nitrogen baffle. The buffer chamber pump was CVC-type PMC 720, with water baffle, and the main chamber pump was CVC-type PMC 720 with water baffle and liquid-nitrogen trap. The pump fluid used was Octoil. In addition to the traps mentioned there was also a thimble-type liquid-nitrogen trap near the detector in the main chamber. The base pressure in all chambers was 5×10^{-7} Torr. Under typical operating conditions helium was let into the source chamber through a liquid-nitrogen trap to a pressure of 2×10^{-4} Torr; the buffer chamber pressure then rose to 10^{-6} Torr, while the main chamber pressure changed less than 1×10^{-7} Torr.

B. Electron Gun

Figure 3 is a schematic diagram of the electron gun as seen by an atom in the beam. The gun is essentially a plane diode, with a hole in the anode A to let electrons enter the field-free region defined by a tube at anode potential. The electrode G was originally intended to provide electrostatic focusing, but in the measurements reported on in this paper G was connected to the anode. The electron beam current was measured by a Faraday cup F with an electrode H biased to suppress secondary electrons. The Faraday cup assembly with its suppressor electrode could be translated in a direction perpendicular to both the electron and atom beams. The electrons were collimated by a vertical magnetic field of approximately 50 G provided by a single large coil outside the vacuum system.

Since the whole gun was immersed in helium gas, the whole of the electron beam was a source of metastable atoms. However, the detector could register only those formed in the region marked S in Fig. 3. This region was the volume defined by the intersection of the electron beam and the set of straight lines passing through both the detector slit and the first beam-defining slit (No. 1 in Fig. 2).

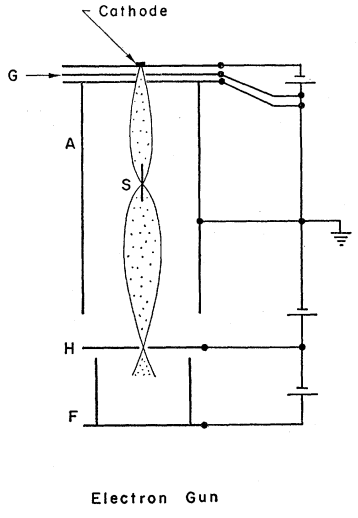

FIG. 3. Schematic diagram of the electron gun.

At a typical electron energy of 20 eV, the pitch of the spiral traced out by an electron in a 50-G field is 1.89 cm, which is close to the distance from the cathode to the center of the atom beam (1.91 cm), so that the 50-G field focused the electrons on the atom beam. Images of the cathode reoccurred periodically along the electron beam. Their spacing was not exactly uniform because of magnetic field inhomogeneities and also because of the suppressor-anode voltage. The net effect was that when the electrons were focused on the atom beam, they were also approximately focused on the suppressor aperture. In Fig. 3 the stippled region is intended to suggest the shape of the electron beam, scalloped by the magnetic field. Under these focusing conditions, which were the operating ones, the current to the Faraday cup was 135 μA, to the suppressor electrode 10 μA, and to the walls of the field-free region less than 1 μA. The electron current density at the sensitive volume was $\sim10^{-2}$ A/cm^2.

The existence of the magnetic focusing effects described above was verified quantitatively by measuring electron beam shapes and metastable signals as a function of electron energy and collimating magnetic field strength. Further details may be found in Ref. 15.

In order that the electron current density at the atom beam be related in a fixed way to the current at the Faraday cup, it was necessary that the spatial distribution of the electron beam be independent of electron energy. According to general scaling laws,[16] this will be so if the magnetic field H and applied electric potential V scale together so that H is proportional to $V^{1/2}$. In addition, if space-charge effects contribute significantly to the electric field seen by an electron, it is also necessary that the current density be proportional to $V^{3/2}$. In our experiment the magnetic field and applied potentials were so scaled together. Since the emission from the cathode was space-charge limited, the current density automatically was proportional to $V^{3/2}$. All observed metastable atom signals were normalized to constant electron current by dividing them by $V^{3/2}$.

The energy width of the electrons could not have had a full width at half-maximum (FWHM) less than 0.3 eV, which is the thermal spread corresponding to the cathode temperature. On the other hand, a retarding-potential measurement gave a FWHM of 0.6 eV; the true width must lie somewhere in between. That inferred from the onset of the 2^3S metastable signal was about 0.5 eV, and this seems to be a reasonable estimate.

The electrodes were made of type-304 stainless steel and were mounted on alumina rods with alumina spacers. The apertures in G and A were 0.13 cm in diameter and 0.13 cm apart. The hole in the suppressor

[15] H. K. Holt, Ph.D. thesis, Yale University, 1965 (unpublished).

[16] J. R. Pierce, *Theory and Design of Electron Beams* (D. Van Nostrand Company, Princeton, New Jersey, 1949), p. 16.

electrode was a slit 0.10 cm wide in the direction of its motion. The interaction volume was 0.668 cm long along the electron beam, 0.016 cm wide and about 0.13 cm long along the atom beam. The latter dimension was determined by the electron beam and so was not as well defined as the others, which were defined by slits. The indirectly heated cathode was of a dispenser type (Philips Metalonics type BP-1A). It was 1.91 cm from the center of the interaction volume and 4.57 cm from the suppressor electrode H.

The suppressor electrode was biased 35 V negative with respect to the Faraday cup and 30 V positive with respect to the anode. The purpose of the latter bias was to keep the interaction region free of reflected electrons from the cup assembly. If present, such electrons worsened the energy spread at the interaction volume, and the advantage obtained by minimizing them overcame any disadvantages due to field penetration.

The gun assembly was enclosed in a type-304 stainless steel oven operated continuously at 300°C to minimize surface oil films.

C. Pressure Dependence of the Signal

The points in Fig. 4 represent measurements of the total metastable signal plotted against the pressure in the source chamber. The pressure was measured by an ion gauge; the gauge was calibrated for air and a factor of 4 was used to correct to helium. Both the magnetic field gradient in the main chamber and electric quenching field in the buffer chamber were off when these data were taken, so the ordinate includes contributions from both singlet and triplet metastables. The peak occurs primarily because at high pressures metastable atoms are scattered out of the beam. If only this process were important and if the scattering cross section were the same for singlets and triplets, the signal as a function of pressure would be represented by a curve of the form $n\exp(-n\sigma x)$, where n is the number density of helium atoms at the pressure in question, σ is the cross section for elastic scattering of metastable helium atoms in ground-state helium, and x is the distance from the interaction volume to the first beam-defining slit (No. 1 in Fig. 2). This theoretical curve, normalized to the experimental peak height, is the dashed line in Fig. 4, with $x=4.76$ cm and $\sigma=1.65\times10^{-14}$ cm^2, a value taken from the work of Stebbings.[17]

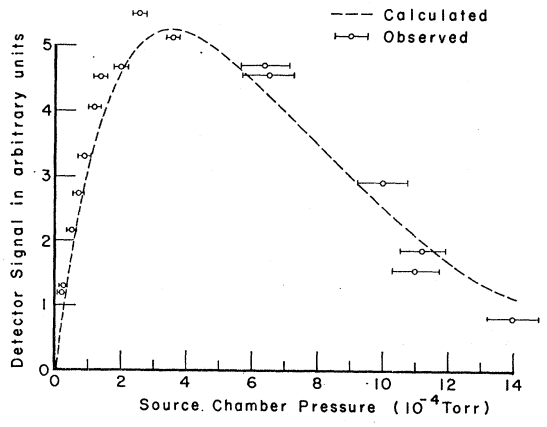

FIG. 4. Pressure dependence of the total metastable signal. Cross-section data were taken at about 2×10^{-4} Torr.

For intensity reasons the cross-section measurements reported in this paper were made at a helium source pressure of 2×10^{-4} Torr, just before the peak of the curve in Fig. 4. At this pressure, 42% of the metastable atoms were scattered out of the beam in the source chamber. (A certain fraction of the detected atoms must also have been scattered *into* the beam. This fraction may be estimated to be less than 10^{-3}.[15])

Since all cross sections were measured relative to that for producing the 2^3S state directly, we did not have to operate in a linear pressure range. However, since the metastable beam was attenuated in the source chamber, a difference between the singlet- and triplet-atom atom-scattering cross sections could lead to an error in a measurement of the 2^1S cross section. One run was made at a lower pressure of 4×10^{-5} Torr in which the attenuation of the metastable beam was only 10%. Comparing the results with data at 2×10^{-4} Torr, it was found that in the range 19.8 to 23 eV the ratio of the singlet-to-triplet electron excitation cross sections was unchanged to within a statistical error of 10%. A brief calculation shows that it may be concluded that the 2^1S and 2^3S cross sections are the same to within $\pm15\%$. This is in agreement with the results of Phelps[18] who found equality to 20%. In the analysis of the 2^1S data, any difference between the two cross sections was neglected.

A possible difficulty could arise in the results of Sec. 3D if it were likely that a triplet metastable were to change its spin in a collision with a ground-state atom. The cross section for this is expected to be small, since by conservation of angular momentum it implies that the spin change must be compensated for by a change in the relative orbital motion. There is also direct experimental evidence that it *is* small. The relaxation time observed in experiments on optical pumping of metastable helium, at a pressure of about 1 Torr, is of order 2×10^{-4} sec,[19] and is believed to be due primarily to effects other than collisions with ground-state helium atoms. However, even if it were due entirely to such collisions it would imply a depolarizing cross section of order 10^{-18} cm^2, which would be unobservable in our experiment.

Another pressure-dependent effect is the contribution to the detector signal of ultraviolet photons at 584 Å from decay of atoms in the 2^1P state. Such photons would constitute an unwanted background, indistinguishable from 2^3S atoms with magnetic quantum

[17] R. F. Stebbings, Proc. Roy. Soc. (London) **A241**, 270 (1957).
[18] A. V. Phelps, Phys. Rev. **99**, 1307 (1955).
[19] F. D. Colegrove and P. A. Franken, Phys. Rev. **119**, 680 (1960).

number zero. However, this background is expected to be small for three reasons:

First, the cross section for making 2^1P atoms in our energy range was measured by Dorrestein to be less than 10% of the metastable signal.[10] Secondly, at 2×10^{-4} Torr only about 5% of the photons made traversed the source chamber without being resonantly scattered. This estimate is based on Holstein's theory of resonant absorption.[20] The contribution from photons scattered *into* the beam is also expected to be small (6% of the direct photon beam).[15] Thirdly, the electron ejection efficiency on tungsten has been measured to be about 15%,[21] or about half that for metastables. The net effect is that at a source pressure of 2×10^{-4} Torr the photon signal is expected to be less than 1/200 the metastable signal and hence negligible. Further details may be found in Ref. 15.

D. Electric Field Region

The electric field in the buffer region B of Fig. 2 was established by a pair of type-304 stainless steel plates 9.84 cm long and 0.053 cm apart. Under typical operating conditions the potential difference V between them was 12 kV, corresponding to a field of 226 kV/cm. Application of this voltage caused the metastable signal to drop, primarily because the electric field coupled the 2^1S state to the 2^1P state, which can decay to the ground state. The magnitude of the drop is a measure of the number of 2^1S metastables in the beam.

Figure 5 shows a typical quenching curve in which the magnitude of the drop is plotted as a function of the square of the applied potential difference. Within the error bars shown, the observed quenching was independent of the sign of V. The dashed line is a theoretical curve with two parameters which have been adjusted to optimize the fit to the experimental points. One of these parameters is the number of singlet metastable atoms.

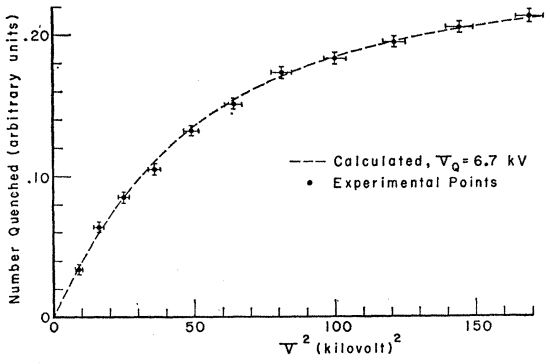

FIG. 5. This curve shows the number of 2^1S metastable atoms quenched by a potential difference of V kilovolts applied across the plates in chamber B of Fig. 2.

The other, V_Q, measures the ease with which metastables are quenched and is calculable from a knowledge of matrix elements, plate dimensions, and the velocity distribution of the atoms in the beam. Such a calculation is described in the Appendix. Its result is a value for V_Q of 6.2 ± 1.2 kV, where the error is due to uncertainties in the electrode geometry, atomic velocity, and matrix elements. The value corresponding to the dashed curve of Fig. 5 is 6.7 ± 0.3 kV, where the error is essentially a measure of how much the dashed curve in Fig. 5 can be distorted and still pass through the experimental points. The agreement is within the quoted errors.

One further possible source of error not included in the above is that charged surface oil films decreased the electric field. We were not able either to prove or disprove this hypothesis.

Cross-section data were taken with 12 kV across the plates. This gave the largest field which could be consistently maintained without breakdown. Using the value 6.7 ± 0.3 kV for the quenching parameter V_Q, it turns out that $(90\pm2)\%$ of the singlets were quenched. This number was then used to correct the observed drop in signal to complete quenching.

E. The Magnetically Deflected Beam and Its Velocity Distribution

The field gradient magnet, located in the main chamber of Fig. 2, was of the conventional two-wire type.[22] It was 15.24 cm long, and the bead had a radius of $a=1.52$ cm. The atom beam was a vertical ribbon passing a distance $z=1.2a$ from the vertical plane containing the two (fictitious) wires. The direction of the field gradient was horizontal. Its magnitude was about 4000 G/cm and it was constant to better than 1% over the atom beam cross section. The points of Fig. 6 represent measurements of detector counting rate plotted as a function of detector position, with the gradient magnet on. Only one-half the deflected beam shape is shown since it was symmetrical. The width of the detector slit was 0.025 cm. The observed deflected beam shape was found to depend somewhat on the source pressure. The points of Fig. 6 were taken at a source pressure of 2.2×10^{-4} Torr (the pressure at which the cross-section data were taken). The reason for the pressure dependence is probably that the velocity distribution of the atom beam depended on source pressure through a number of effects. One of these effects is the velocity dependence of the elastic scattering cross section of metastable helium atoms in helium. It was estimated[15] that this could account for about half the observed pressure dependence. A further complicating feature is that the gas in the source chamber saw three different temperatures: the inlet and walls were at room temperature, the oven was at 300°C, while

[20] T. Holstein, Phys. Rev. **72**, 1212 (1947).
[21] W. C. Walker, N. Wainfan, and G. L. Weissler, J. Appl. Phys. **26**, 1366 (1955).
[22] P. Kusch and V. W. Hughes, in *Encyclopedia of Physics*, edited by S. Flügge (Springer Verlag, Berlin, 1959), Vol. 37, Chap. 1, p. 43.

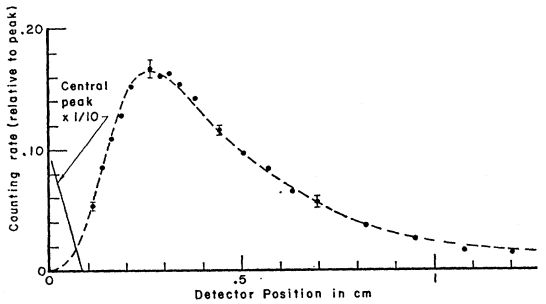

FIG. 6. The magnetically deflected beam shape. Only half of the whole distribution is shown since it was symmetric.

under one open end of the oven was a liquid-nitrogen trap.

A knowledge of the atomic velocity distribution was not required for the cross-section measurements. It was used only in obtaining the calculated value of the electric field quenching parameter V_Q. Since the experimentally determined value of V_Q (6.7 ± 0.3 kV) was used in making the 10% correction to high field strength the uncertainty in the velocity distribution did not affect the measured 2^1S cross section.

Nevertheless, it is interesting to compare the observed velocity distribution with that expected theoretically. Experimentally, it was found that for source pressures in the range 4×10^{-5} to 3.8×10^{-4} Torr, the observed deflected beam shapes could be fitted by assuming the velocity distribution of the metastable atoms to be given by the equation

$$f(v)dv=2(v/\alpha)^3\exp(-v^2/\alpha^2)dv/\alpha \qquad (1)$$

with the parameter α being a function of pressure. In Eq. (1), $f(v)dv$ is the contribution to the detector counting rate made by atoms whose velocities were in the range dv about v. The parameter α varied from 1.12×10^5 cm/sec at 4×10^{-5} Torr to 1.23×10^5 cm/sec at 3.8×10^{-4} Torr. The corresponding deflections of atoms with velocity α varied from 0.86 to 0.71 cm. The dashed curve in Fig. 6 was computed from Eq. (1) with $\alpha=1.19\times10^5$ cm/sec. It was estimated that this value could be changed by $\pm0.09\times10^5$ cm/sec without substantially affecting the fit to the experimental points of Fig. 6.

From a theoretical point of view the usually quoted[23] velocity distribution of atoms effusing from a slit is a "v^3" one; two powers of v come from the Maxwell distribution, the other from the rate at which atoms bombard the slit. In our case, this bombardment rate is replaced by the rate at which the electron gun makes metastable atoms and is not dependent on atom velocity (this is because the atom velocity was small, $\sim10^5$ cm/sec, compared to the electron velocity $\sim10^8$ cm/sec). Hence the expected velocity distribution is a "v^2" one,[24] not a "v^3" one. We regard the "v^3" distribution which fits the data of Fig. 6 as just a convenient description of the facts, with the departure from a "v^2" distribution being due to the effects mentioned above (velocity dependence of the elastic scattering cross section, together with a poorly defined temperature in the source region).

F. Detector

The detector was a Bendix type-M306 electron multiplier. In this detector, metastable atoms strike a tungsten surface and eject electrons by the Auger effect. The ejected electrons are multiplied by the dynode structure and the output pulse is counted. Typical counting rates were 10 to 10^3/sec. The detector was insensitive to ground-state helium atoms. Since our cross-section measurements were relative, knowledge of the detector efficiency was not required. However, it is useful to have a rough idea of its value. An upper limit is provided by the probability for the Auger ejection of an electron by a metastable atom from tungsten. This has not been measured but it is expected[25] that gold and tungsten should not be too different, and for gold Stebbings[17] found an efficiency of 0.29 ± 0.03.

The actual detector efficiency may have been less because not all the ejected electrons were caught up by the multiplier structure, and not all the pulses at the multiplier output were recorded by the electronics. The biases on the multiplier were empirically adjusted to give maximum counting rate; with the anode very close to ground potential, the cathode was biased at -1900 V and the grid at -1100 V. The voltage drop across the dynode strip was 1700 V and the anode end of the field strip was grounded.

The height spectrum of the output pulses was measured and the amplifier discriminator set to reject the small regeneration pulses. It was estimated that less than 20% of the true output pulses were lost.

The dimensions of the tungsten cathode were 1.83 cm $\times$1.56 cm. However, not all of it was used. A vertical slit 1.59 cm $\times$0.025 cm was mounted in front. The whole detector assembly, with slit, could be moved under vacuum in a horizontal direction perpendicular to the direction of the atomic beam.

3. RESULTS

A. Total Metastable Cross Section

The total metastable cross section was measured by turning off the quenching and deflecting fields, setting the detector at the center of the undeflected beam shape, and measuring the counting rate as a function of electron energy. This cross section has been measured

[23] N. F. Ramsey, *Molecular Beams* (Oxford University Press, London, 1956), p. 20.

[24] Except for small corrections due to recoil of the electron. These are 2% at most.

[25] H. D. Hagstrum, Phys. Rev. **96**, 325 (1954); **96**, 336 (1954).

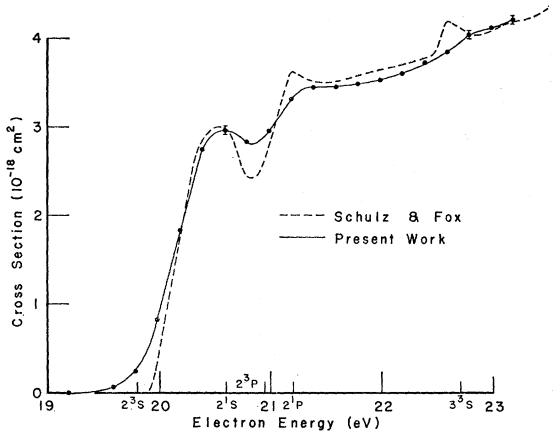

FIG. 7. The total cross section for production of metastable (2^3S and 2^1S) states, including cascade effects. The cross-section scale was adjusted so that the first peak in the curve was exactly 3×10^{-18} cm^2. Error bars shown are statistical only.

before[2,3,10] and our measurement was made as a check on the apparatus.

The results are shown in Fig. 7. The error bars show the statistical error (± two times the dispersion). The dashed curve represents the results of Schulz and Fox[2] taken with an energy resolution of about 0.1 eV. The agreement appears satisfactory if allowance is made for the difference in energy widths.

The thresholds of the various states are marked on the abscissa of Fig. 7. From these it is evident that the first peak is due to excitation of the 2^3S state. The value of the cross section at this peak has been measured by Schulz and Fox,[2] who obtained $(4\pm1.2)\times10^{-18}$ cm^2, and by Fleming and Higginson,[3] who obtained $(2.6\pm0.4)\times10^{-18}$ cm^2. We measured our cross sections relative to this peak, and took the height to be 3.0×10^{-18} cm^2. The error in this value is estimated to be $\pm0.7\times10^{-18}$ cm^2. However, the error bars in Figs. 7, 8, 9, and 10 do not take this into account. The figures were drawn using a peak value of exactly 3.0×10^{-18} cm^2.

It should be noted that the apparent thresholds observed were not at the spectroscopic values shown in Fig. 7, but actually about 1.82 V higher. This discrepancy was due to space charge and contact potential effects and the curve shown in Fig. 7 was arbitrarily shifted to compensate for these. The same shift has been applied to the energy scales of all the figures.

B. 2^1S Cross Section

The 2^1S cross section was measured by setting the detector in the center of the beam and measuring the counting rate as a function of electron energy both with the electric quenching field on and off. When corrected to high quench field, the difference is the 2^1S cross section shown in Fig. 8. The error flags shown are due to statistical errors and the quenching uncertainty of Sec. 2D, the two being approximately equal. The contribution of cascade from the 2^1P state to the observed current of 2^1S atoms was negligible since the 2^1P state decays overwhelmingly to the ground state.

The solid curve shows the 2^1S cross-section curve calculated by Marriott.[4] Marriott's calculation consisted of an exact numerical solution of the approximate equations obtained for each value of the orbital angular momentum l by expanding in terms of atomic eigenfunctions and neglecting all terms involving states other than 1^1S, 2^1S, and 2^3S. Values of l from 0 to 3 were included. The shape of his calculated curve agrees well with the measured one, but it is high by approximately a factor 3.3.

The 2^1S cross section has also been calculated by Massey and Moiseiwitsch,[5] using a distorted-wave method in which the coupling between the singlet- and triplet-metastable levels was neglected. Their calculation is not expected to be valid near threshold, but its low-energy limit is also shown on Fig. 8.

No direct measurements of the total 2^1S cross section have been reported in this energy range. However, the result of Fig. 8 may be compared with the cross section obtained indirectly by Frost and Phelps.[26] Frost and Phelps' values are about a factor 3 greater than the values shown in Fig. 8.

C. The 2^3S+2^3P Cross Section

The quenching of the 2^1S state also yields the sum of the 2^3S and 2^3P cross sections. It is assumed that for the reasons discussed at the end of Sec. 2C, the excitation of the 2^1P state can be neglected. The result is the upper set of experimental points in Fig. 9 with the error flags again being due to statistical errors and quenching uncertainties.

The second set of experimental points is an estimate of the 2^3P cross section. This was obtained by first

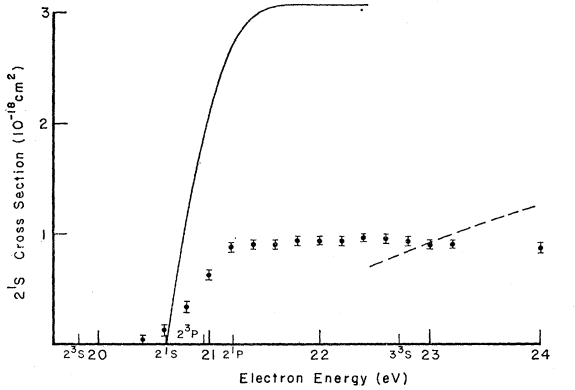

FIG. 8. The total cross section for production of the 2^1S state, with the cross-section scale adjusted so that the 2^3S peak is exactly 3×10^{-18} cm^2. Error bars are partly statistical and partly due to quenching uncertainties. The solid curve is a calculation by Marriott (Ref. 4), the dashed one by Massey and Moiseiwitsch (Ref. 5).

[26] L. S. Frost and A. V. Phelps, Westinghouse Research Laboratory Report 6-94439-6-R3 1957 (unpublished).

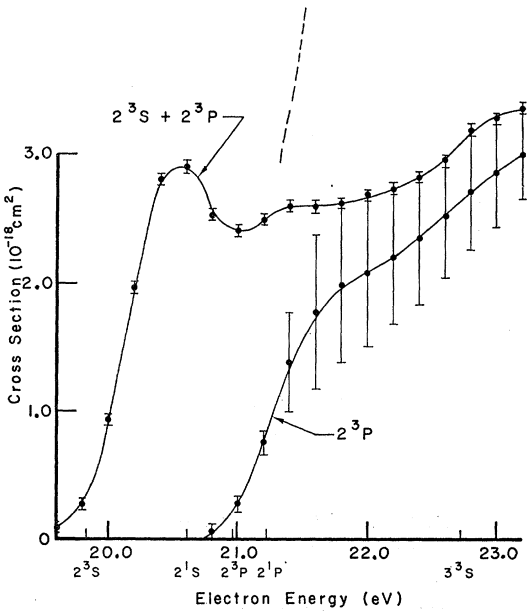

FIG. 9. The sum of the 2^3S and 2^3P cross sections, together with an estimate of the 2^3P cross section. The cross-section scale was adjusted so that the peak of the 2^3S cross section was exactly 3×10^{-18} cm². The dashed line is a theoretical curve due to Massey and Moiseiwitsch (Ref. 6).

estimating the 2^3S cross section and subtracting from the sum. The large error bars are dominantly due to the uncertainty of the 2^3S estimate, as described below.

Above the 2^3P threshold, the only direct measurements of the 2^3S cross section have been by detection of the inelastically scattered electrons. In the experiments reported to date, differential cross sections have been obtained at 72°[13] and at 0°.[14] These two experimental results differ in that with increasing energy the cross section at 0° drops to zero faster than it does at 72°, presumably because the angular distribution is not isotropic. Theoretical calculations of the total cross section have been carried out by Marriott[4] and Massey and Moiseiwitsch.[5] Below the 2^1S threshold both calculations overestimate the experimental results of Fig. 7 by a factor 2 to 3. The total 2^3S cross section adopted was an average of the two measurements of differential cross sections, with error bars large enough to include both. The result was not inconsistent with the theoretical calculations if the latter were normalized to 3×10^{-18} cm² at the peak.

The 2^3P cross section obtained may be compared with the results of Massey and Moisiewitsch who used a distorted-wave method.[6] Their result is not expected to be valid near threshold but its low-energy limit is shown as the dashed line of Fig. 9. It is evidently much too large.

D. Populations of Magnetic Substates

The following is a summary of what should be expected on theoretical grounds. In general, when an unpolarized electron beam excites a helium atom, states differing only in the sign of the magnetic quantum number m are equally populated, the axis of quantization Z being taken along the electron velocity. This follows from the invariance of the Hamiltonian under the operations of parity and rotation.

More detailed conclusions can be drawn from the fact that $\mathbf{l}\cdot\mathbf{s}$ terms in the Hamiltonian are small compared to electrostatic terms. For helium, the largest fine-structure separation occurs in the 2^3P state and is about 10^4 Mc/sec, which corresponds to a time of 10^{-10} sec. This time is long compared to the time of a collision, which may be taken to be at most a lifetime inferred from the widths of the resonances seen in electron helium scattering,[13,14,27,28] or less than 10^{-13} sec. Hence the fine-structure interaction may be switched off during the collision, which then proceeds through the Coulomb force.

Since a Hamiltonian with only kinetic-energy and electrostatic terms conserves spin and orbital angular momentum separately, and since the initial spin state is known, the final-state spin population may be calculated in terms of vector-coupling coefficients. The result is that states of the excited atom differing only in M_S are equally populated ($M_S\hbar$ being the Z component of the spin of the excited atom); this is to be expected since the Coulomb force does not act on the spin coordinate, and the initial unpolarized spin state does not single out any direction in spin space.

The total orbital angular momentum of the whole system, consisting of electron plus atom, is not well defined in general so equally simple conclusions concerning the populations of the various M_L states cannot be drawn ($M_L\hbar$ being the Z component of the orbital angular momentum in the final state of the excited atom).

These conclusions assume an electrostatic Hamiltonian; the assumption is valid only for times short compared to the typical fine-structure time of 10^{-10} sec. In particular, the 2^3P state decays with a lifetime of 10^{-7} sec,[29] and hence will decay long after the fine-structure terms in the Hamiltonian have had time to act on the newly created state. These $\mathbf{l}\cdot\mathbf{s}$ terms will force the atom to decay out of its energy eigenstates, that is, states with definite J and M_J, where J refers to the total angular momentum. Hence, the atom decays out of an incoherent mixture of J M_J states populated according to the squares of vector coupling coefficients relating a J M_J state to an M_L M_S state.

According to this picture, if only those 2^3S atoms are considered which are made through the 2^3P state, then the relative populations of the final magnetic substates are calculable in terms of cross sections Q_{M_L} for popu-

[27] C. E. Kuyatt, J. A. Simpson, and S. R. Mielczarek, Phys. Rev. 138, A385 (1965).
[28] G. J. Schulz, Phys. Rev. 136, A650 (1964).
[29] W. R. Bennett, P. J. Kindlmann, and G. N. Mercer, in Appl. Opt. Suppl. Chem. Lasers 2, 34 (1965).

lating that magnetic substate of the 2^3P level which has Z component of orbital angular momentum $M_L\hbar$ and Z component of spin $M_s\hbar$ (with the Q's being independent of M_s). The resulting population distribution (N_{-1},N_0, N_1) among the magnetic substates of the 2^3S state may be described by the conventional polarization parameters for a spin-1 particle[30]; since $N_{-1}=N_1$ all of these are zero except the tensor polarization[31] P_{33}, defined as

$$P_{33}\equiv\frac{N_{-1}-2N_0+N_1}{N_{-1}+N_0+N_1}=\frac{2(N_1-N_0)}{N_0+2N_1}. \quad (2)$$

In terms of the cross sections Q_0 and $Q_1(=Q_{-1})$, the tensor polarization is given by

$$P_{33}=(5/18)2(Q_1-Q_0)/(Q_0+2Q_1). \quad (3)$$

P_{33} is closely related to the (vector) polarization P of the light emitted in the $2^3P\rightarrow 2^3S$ decay, where P is defined as in Ref. 32. The exact relation is

$$P_{33}=-4P/(3-P);\ P=-3P_{33}/(4-P_{33}). \quad (4)$$

It may also be noted that in the particular case of the $2^3P\rightarrow 2^3S$ decay, where the final state has spin 1, like a photon, P is also related to the populations N_0, $N_{\pm1}$ through the equation

$$P=(N_0-N_1)/(N_0+N_1). \quad (5)$$

Although the ratio Q_1/Q_0 is not easy to calculate in general, there are at least two special cases in which it may easily be obtained. One of these arises at energies near a resonant state of the negative helium ion. In this case the total orbital angular momentum will be well defined, and Q_1/Q_0 is calculable in terms of vector-coupling coefficients. This case will be discussed in Sec. 4.

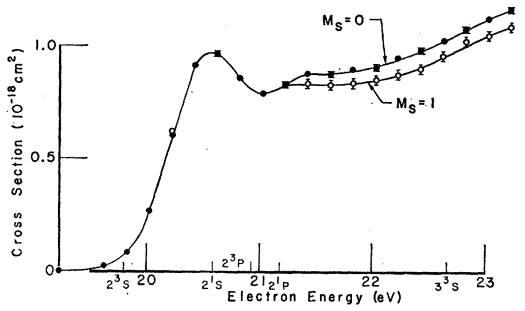

FIG. 10. Magnetically analyzed cross sections for exciting the 2^3S state, both directly and by cascade from the 2^3P state. The cross-section scale is adjusted so that the peak of the total 2^3S cross section is 3×10^{-18} cm^2.

[30] L. J. B. Goldfarb, Nucl. Phys. **7**, 622 (1958),

[31] A similar polarization parameter for spin-1 particles is defined in Ref. 19. There it is called the alignment A and is equal to $-\frac{1}{2}P_{33}$.

[32] I. Percival and M. J. Seaton, Phil. Trans. Roy. Soc. (London) **A251**, 113 (1958).

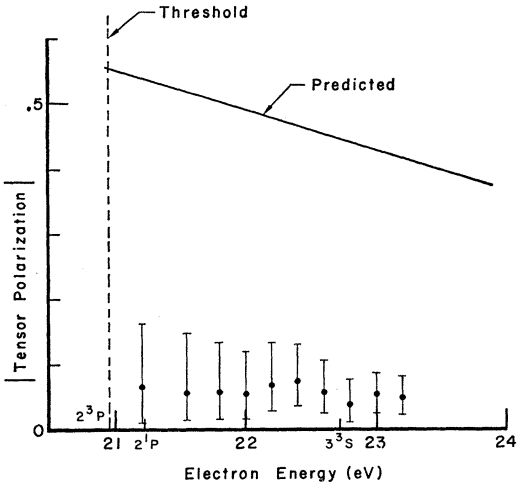

FIG. 11. Measured tensor polarization of those 2^3S atoms made by cascade from the 2^3P state.

The other special case arises at the threshold for 2^3P production. At this energy the scattered electron is emitted in an S wave, and all the orbital angular momentum of the final state will be in the excited atom. Since the initial state of the whole system has no orbital angular momentum about the Z axis, it may be concluded that at threshold $Q_1/Q_0=0$, and from Eqs. (3) and (4), $P_{33}=-5/9$, $P=15/41$.

As is well known, the measured polarization of collision light is typically much less than the calculated threshold value.[11,33] The particular case of the near-threshold polarization of the $2^3P\rightarrow 2^3S$ light in helium has not been measured. Our measurements on the relative populations of the magnetic substates of the 2^3S state are equivalent to a measurement of this polarization, but carried out by quite different means. The measured excitation functions are shown in Fig. 10.

The data of Fig. 10 were taken with both quenching and deflecting fields on; the plotted points are the cross sections for exciting the $M_s=0$ and $M_s=\pm1$ magnetic substates of the 2^3S state including cascade from the 2^3P state, the two measured curves being independently normalized to the 2^3S peak. At energies above the 2^3P threshold the two curves differ, with $M_s=0$ being more likely than $M_s=1$. This is ascribed to the polarization effects described above; using the 2^3P cross section of Fig. 9, the measured tensor polarization is shown in Fig. 11, which also show the theoretically expected value according to the distorted-wave calculation of Massey and Moiseiwitsch.[6] The measured tensor polarization is less by approximately a factor 6 than the predicted threshold alignment. This result is discussed in Sec. 4.

[33] D. W. O. Heddle and R. G. W. Keesing, *Abstracts of Papers at IVth International Conference on the Physics of Electronic and Atomic Collisions* (Science Bookcrafters, Inc., Hastings-on-Hudson, New York, 1965), p. 382.

4. DISCUSSION

The data of Fig. 11 were taken with a poorer energy resolution than some of the optical measurements[11,34] and, in addition, there was the complicating feature that the 2^3P cross section is not well known. However, it seems clear that more than 0.5 V above threshold the tensor polarization is much less than the threshold value; a value of $-5/9$ for the tensor polarization would imply that the separation of two curves of Fig. 10 should be approximately six times greater than shown. A number of explanations may be advanced for the low value of the observed tensor polarization.

One possibility is that there is some spurious experimental effect which tends to equalize the population of 2^3P or 2^3S magnetic substates. In the literature on polarization measurements, among the effects considered there have been included the elastic scattering of electrons, atom-atom scattering, cascade from higher states, trapping of resonance radiation, lack of collimation of the electron beam, and dependence of the polarization on the magnetic field. These effects will now be considered.

Elastic electron scattering can decrease the observed tensor polarization because it leads to a flux of electrons travelling in the wrong direction. Such effects have been discussed in particular by McFarland.[34] In our case, assuming the elastic-scattering cross section at 20 eV to be 2.5×10^{-16} cm^2,[35] the probability that an electron was elastically scattered in the gun is less than 1%. The fraction of electrons travelling in a direction substantially different from the nominal one will be even less; it does not seem possible that this effect could decrease the alignment by more than a few percent, even taking path length differences into account.

The effects of atom-atom scattering would also appear to be negligible. At 2×10^{-4} Torr, the probability that a 2^3P atom collided with a helium atom before it decayed is less than 10^{-3}, assuming the cross section to be 10^{-14} cm^2. Once the 2^3P atom had decayed to the 2^3S state, the probability that the relative populations of the 2^3S magnetic substates were changed is less than 10^{-4}, according to the considerations of Sec. 2C.

Population of the 2^3P state by cascade from higher ones may be ruled out in the present experiment since the electron energy was kept below the $n=3$ threshold.

Resonance trapping could not have been a factor since the results of Fig. 11 are concerned with triplet states, not optically connected to the ground state.

The measured tensor polarization was less than the true tensor polarization because the electron beam was not perfectly collimated. It may be shown that if $(P_{33})_0$ is the tensor polarization produced by an electron travelling parallel to the magnetic field in the interaction volume, then the tensor polarization P_{33} produced by an electron whose velocity makes an angle θ with the field is given by

$$P_{33}=(P_{33})_0\,\tfrac{1}{2}(3\cos^2\theta-1). \tag{6}$$

In this experiment the angle θ lay in the range zero to 0.25 rad. Assuming that all angles in this range were equally likely, it may be shown by a brief calculation that the measured tensor polarization could not have been less than the true one by more than 5%, which is small compared to the factor 6 of Fig. 11.

In principle, the measured tensor polarization depends on the strength of the magnetic field through the decoupling this introduces between the spin and orbital angular momenta in the 2^3P state. The characteristic field strengths involved are of order 1640 G, and at 50 G the effect on the tensor polarization is calculated to be only about 1%.

If it is accepted that there were no significant spurious experimental effects tending to lower the measured tensor polarization, the question arises of how to interpret the results of Fig. 11. Since resonances appear to be important in determining cross sections, it seems natural to consider our results from this point of view. Measurements of tensor polarization can play a role similar to (but not necessarily equivalent to) measurements of angular distribution in distinguishing between contributions of different angular momenta to the total cross section. This may be seen as follows.

In general, all cross sections may be expressed in terms of elements of the collision matrix. Neglecting spin-dependent forces, these matrix elements may be denoted by $S_{Ll'}$, where $L(L+1)\hbar^2$ is the square of the total-orbital angular momentum of the three electrons, and $l'(l'+1)\hbar^2$ is the square of the orbital angular momentum of the scattered electron relative to the residual atom. (The total spin quantum number is always $\frac{1}{2}$). Since the ground state of the helium atom has no orbital angular momentum, the quantum number L is equal to l, where $l(l+1)\hbar^2$ is the square of the orbital angular momentum of the incoming electron relative to the atom, and the parity of the whole system of 3 electrons is $(-1)^L$. Since the $2P$ state has odd parity, it follows that L and l' must differ by 1.

The total cross section σ for exciting the 2^3P state may be written as the sum of partial cross sections $\sigma_{Ll'}$ defined by the equation

$$\sigma=\sum_{Ll'}\sigma_{Ll'}=\frac{\pi}{k^2}\sum_{Ll'}(2L+1)|S_{Ll'}|^2, \tag{7}$$

where $\hbar k$ is the momentum of the incoming electron. The tensor polarization may also be expressed in terms of the $S_{Ll'}$; the resulting formula is cumbersome, but some of the essential features are shown in Table II, which lists the "partial-tensor polarizations" $(P_{33})_{Ll'}$ obtained by putting all $S_{Ll'}$ equal to zero except one.

Near a resonance with a definite value of L, only the corresponding row of Table II need be considered; the

[34] R. H. McFarland, Phys. Rev. 133, A986 (1964).
[35] D. E. Golden and H. W. Bandel, Phys. Rev. 138, A14 (1965).

TABLE II. Possible values of tensor polarization $(P_{33})_{Ll'}$.

$L\backslash l'$	0	1	2	3
0	···	0	···	···
1	−10/18	···	−1/18	···
2	···	−5/18	···	−5/63
3	···	···	−4/18	···

observed tensor polarization will then be a linear combination of the entries in that row, with coefficients $\sigma_{Ll'}/\sigma$,[36] i.e., it will depend only on the absolute squares of two scattering matrix elements. From a measurement of the tensor polarization, the ratio of the two squares may be deduced. If the total cross section were also measured, the values of the squares themselves may be found (or, equivalently, two reduced widths obtained).

At energies between resonances the situation is more complicted; the general expression for the tensor polarization contains interference terms between matrix elements $S_{Ll'}$ having the same l', i.e., between entries in any one column of Table II. The magnitude of these interference terms need not be small compared to the entries of Table II. There is of course one nonresonant energy at which the expression for the tensor polarization becomes simple, and that is at the 2^3P threshold where all the $S_{Ll'}$ become zero except S_{10}, and the tensor polarization assumes the value −10/18.

The measurements of Fig. 11 were originally motivated by a polarization "anomaly." However, from the point of view of the preceding discussion, there is nothing surprising about the "low" value of tensor polarization obtained. It is consistent with many possibilities; for example, the ^2S resonance at 19.3 eV may dominate the 2^3P cross section in the energy range of Fig. 11, or the matrix element S_{12} may be important, corresponding to a ^2P resonance which emits a d-wave electron. Interference between ^2S and ^2P resonances could also produce the tensor polarization of Fig. 11. About the only possibility which is clearly excluded experimentally is that the 2^3P cross section be dominated by the scattering matrix element S_{10}. Although this is the only matrix element to survive at threshold, the existence of resonances[13,14,27,28] about 0.1 eV wide (or less) in the energy range of Fig. 11 implies that the scattering matrix elements can change substantially over several tenths of an electron volt, so it is not necessarily surprising that half a volt above threshold S_{10} does not dominate the 2^3P cross section.

ACKNOWLEDGMENT

We wish to thank Professor V. W. Hughes for originally suggesting this problem to us and for his advice and encouragement.

[36] However, the polarization of the $2^3P \rightarrow 2^3S$ collision light is not so simply related to partial polarizations $P_{Ll'}$.

APPENDIX: QUENCHING OF THE 2^1S STATE OF HELIUM BY AN ELECTRIC FIELD

In this Appendix, the rate at which a singlet-metastable atom decays in an electric field will be calculated to lowest order of perturbation theory (i.e., to terms quadratic in the field strength.)

In a constant, uniform, electric field of magnitude F directed along the z axis, the perturbed 2^1S wave function $u'(2^1S)$ may be written

$$u'(2^1S)=u(2^1S)+\sum_{n=2}^{\infty}\frac{\langle u(n^1P)|eFz|u(2^1S)\rangle}{E(2^1S)-E(n^1P)}u(n^1P)+\cdots, \quad \text{(A1)}$$

where all the u's and E's represent eigenfunctions and eigenvalues of the unperturbed Hamiltonian. The sum includes an integration over the continuum. This perturbed 2^1S state decays to the ground state at a rate γ given by the usual formula of time-dependent perturbation theory,

$$\gamma=\frac{2\pi}{3}\alpha^3\nu_0\left(\frac{E'(2^1S)-E(1^1S)}{\mathrm{Ry}}\right)^3\left|\left\langle u'(2^1S)\frac{z}{a_0}u(1^1S)\right\rangle\right|^2, \quad \text{(A2)}$$

where α is the fine-structure constant, a_0 is the Bohr radius, $E'(2^1S)$ is the Stark shifted energy of 2^1S state, Ry is the Rydberg energy (13.61 eV), and ν_0 is the Rydberg frequency (i.e., $h\nu_0=\mathrm{Ry}$).

Since the matrix element of z in Eq. (A2) will be proportional to F in lowest order, and γ is required only to order F^2, the perturbed energy $E'(2^1S)$ in Eq. (A2) may be replaced by its unperturbed value $E(2^1S)$. Substituting (A1) into (A2) then leads to an expression for γ in terms of matrix elements of z:

$$\gamma=\frac{2\pi}{3}\alpha^3\nu_0\left(\frac{E(2^1S)-E(1^1S)}{\mathrm{Ry}}\right)^3(eFa_0)^2\times\left|\sum_{n=2}^{\infty}\frac{\langle u(2^1S)|z/a_0|u(n^1P)\rangle\langle u(n^1P)|z/a_0|u(1^1S)\rangle}{E(2^1S)-E(n^1P)}\right|^2. \quad \text{(A3)}$$

In calculating γ from this expression, we used the oscillator strengths shown in Table III. For the m^1S to n^1P transitions of interest, the oscillator strength f is related to the matrix element of z/a_0 through the equation

$$f=[[E(n^1P)-E(m^1S)]/\mathrm{Ry}]\times\langle u(n^1P)|z/a_0|u(m^1S)\rangle^2. \quad \text{(A4)}$$

In Table III, for $n=2$, 3 the oscillator strengths are those calculated by Schiff and Pekeris.[37] For the other

[37] B. Schiff and C. L. Pekeris, Phys. Rev. 134, A638 (1964).

TABLE III. Oscillator strengths f in helium.

Transition	f (absorption)	Transition	f (absorption)
1^1S-2^1P	0.27616±0.00001	2^1S-2^1P	0.3764±0.0002
3^1P	0.0734±0.0001	3^1P	0.1514±0.0002
4^1P	0.032	4^1P	0.051±0.018
5^1P	0.016	5^1P	0.025±0.006
6^1P	0.0093	6^1P	0.012
7^1P	0.0058	7^1P	0.015±0.004
$>7^1P$	hydrogenic	$>7^1P$	hydrogenic

$n^1P \rightarrow 2^1S$ transitions the oscillator strengths were calculated from the lifetime measurements of Bennett *et al.*,[29] except for $n=6$, which these authors did not measure. For $n=6$ the oscillator strength shown in Table III was taken from the compilation of Dalgarno and Kingston.[38] In the case of $n^1P \rightarrow 1^1S$ transitions with $n>3$ the oscillator strengths are those adopted by Dalgarno and Lynn.[39] for $n>7$, including the continuum, hydrogen oscillator strengths were used.[40]

The errors shown in Table III are those quoted by the respective sources. The errors in all the other oscillator strengths were assumed to be ±25%, a figure arrived at by comparing the results of different calculations.

An oscillator strength determines only the magnitude of a matrix element but not its sign. The relative signs are required in Eq. (A3). It was assumed that the signs are correctly given by a calculation using hydrogenic wave functions. With this assumption, all matrix elements have the same sign except for $\langle u(2^1S)|z/a_0|u(2^1P)\rangle$, which has the opposite sign. This is by far the largest matrix element, so that inclusion of coupling to states with $n>2$ tends to decrease the decay rate.

[38] A. Dalgarno and A. E. Kingston, Proc. Phys. Soc. (London) **72**, 1053 (1958).
[39] A. Dalgarno and N. Lynn, Proc. Phys. Soc. (London) **A70**, 802 (1957).
[40] H. A. Bethe and E. E. Salpeter, *Quantum Mechanics of One and Two Electron Atoms* (Academic Press Inc., New York, 1957), Sec. 63, p. 264.

Using the oscillator strengths of Table III, together with the values of the fundamental constants and the energy levels of helium, the value of γ obtained is

$$\gamma=(0.89\pm0.04)F^2 \text{ sec}^{-1}, \tag{A5}$$

where F is field strength in kV/cm. The error is due to uncertainties in the oscillator strengths. Terms in Eq. (A3) with $n>2$ contribute about 20% to the calculated value of γ.

The value of V_Q in Sec. 2D will now be obtained. For a given decay rate γ, the attenuation of a 2^1S beam in passing through the electric field region with a definite velocity v is $\exp(-\gamma t)$, where t is the transit time. The velocity distribution is given by Eq. (1). For a field length l, the observed attenuation A is then given by the integral

$$A=\int_0^\infty \exp(-\gamma l/v)f(v)\,dv \tag{A6}$$

which is a function only of the dimensionless parameter $\gamma l/\alpha$ and is approximately equal to $\exp(-\gamma l/\alpha)$. Since the decay rate depends on the square of the applied electric field, the dimensionless parameter $\gamma l/\alpha$ may be written as V^2/V_Q^2, where V is the potential difference across the plates and V_Q is a characteristic voltage. In terms of l, α, d(the separation between the plates), and the coefficient 0.89 of Eq. (A5), V_Q is given by

$$V_Q=d\left(\frac{\alpha}{l\times0.89}\right)^{1/2}. \tag{A7}$$

For $l=9.84\pm0.3$ cm, $d=0.053\pm0.005$ cm, and $\alpha=(1.19\pm0.09)\times10^5$ cm/sec, V_Q becomes 6.2±1.2 kV/cm. The largest single source of error is the uncertainty in the plate separation d.